Ecological Indicators 54 (2015) 238–245

Contents lists available at ScienceDirect

Ecological Indicators

journal homepage: www.elsevier.com/locate/ecolind

An interval fuzzy model for magnetic biomonitoring using the specie *Tillandsia recurvata* L

Mauro A.E. Chaparro A.E.[a,b,*], Marcos A.E. Chaparro[a], A.G. Castañeda Miranda[c], H.N. Böhnel[c], A.M. Sinito[a]

[a] Centro de Investigaciones en Física e Ingeniería del Centro de la Provincia de Buenos Aires (CIFICEN, CONICET-UNCPBA), Pinto 399, 7000 Tandil, Argentina
[b] Departamento de Matemáticas, Facultad de Ciencias Exactas y Naturales UNMDP, Funes 3385, 7600 Mar del Plata, Argentina
[c] Centro de Geociencias, UNAM, Blvd. Juriquilla 3001, 76230 Juriquilla, Querétaro, Mexico

ARTICLE INFO

Article history:
Received 18 June 2014
Received in revised form 9 February 2015
Accepted 10 February 2015

Keywords:
Biomonitoring, Fuzzy *c*-means clustering
Model
Magnetic parameters
Pollution

ABSTRACT

Studies of magnetic monitoring for assessing air pollution have been proposed as alternative and complimentary of chemical methods. Such magnetic studies provide measurements at low cost and relative promptness. In this work, we present and apply a methodology to build an interval fuzzy model, which calculates the Tomlinson pollution load index (PLI). The input variables for the model are magnetic parameters relative to magnetic concentration, grain size and mineralogy. The model aims to two purposes, on one hand, to calculate the values of PLI only using magnetic variables and, on the other hand, to analyze the relationship between magnetic and chemical variables. The studied dataset was obtained from measurements of the biomonitor *Tillandsia recurvata L.* in a Mexican urban area (Santiago de Querétaro). The best model was selected from a total of about half a million possible models using a fitness measure (RIF). The model yields a satisfactory approximation of the PLI data and it was concluded that PLI increases with relation to: an increase in concentration of magnetic materials, an additional contribution to the magnetic signal of paramagnetic materials, and an increase in size of magnetic grains.

1. Introduction

The use of magnetic parameters represents a complementary and alternative tool for magnetic monitoring to assess pollution in areas of interest. It is noteworthy that low cost and relative promptness are features of magnetic methods unlike those of other methods.

The association of the presence of magnetic fractions of atmospheric dusts and ashes generated from industrial combustion or vehicles and the generation of magnetic particles and heavy metals has been shown by several authors (Kapicka et al., 1999; Petrovský et al., 2000; Kukier et al., 2003; Evans and Heller, 2003). Studies of air pollution based on the magnetic properties of vegetation samples – tree leaves, needles, tree ring cores, mosses, lichen – have been carried out since the 1990s (Flanders, 1994; Matzka and Maher, 1999; Jordanova et al., 2003; Moreno et al., 2003; Hanesch et al., 2003; Gautam et al., 2005; Lehndorff et al., 2006; Maher, 2008; Zhang et al., 2008, 2012; Jordanova et al., 2010; Fabian et al., 2011; Salo et al., 2012; Chaparro et al., 2013; Castañeda-Miranda, 2014; Aguilar-Reyes et al., 2012). These works have demonstrated their potential as passive dust collectors and therefore for magnetic monitoring in areas of interest.

In this contribution, data obtained from the epiphytic *Tillandsia recurvata* L. was selected due to its availability in the metropolitan area of Santiago de Querétaro, Mexico. The epiphytic plants are efficient air pollution biomonitors because they obtain their nutrients from the atmosphere and have minimum contact with the earth (Wannaz et al., 2006).

The relationship between magnetic parameters and chemical elements have been studied by several authors in lake sediments (Petrovský et al., 1998; Chaparro et al., 2008), soils (Spiteri, 2005; Chaparro et al., 2007; Morton-Bermea et al., 2009), stream sediments (Desenfant et al., 2004; Chaparro et al., 2006), biomonitors (Georgeaud et al., 1997; Fabian et al., 2011; Salo et al., 2012; Chaparro et al., 2013), atmospheric dusts (Ng et al., 2003; Castañeda-Miranda et al., 2014) and automobile emission (Lu et al., 2005; Marié et al., 2010). These studies indicate that the relationship may not be generalized but is particular for each environment studied. In particular, in our previous studies (Chaparro et al., 2011, 2012), multivariate statistical analyses and fuzzy tools were used for magnetic monitoring in soils, stream and river sediments,

* Corresponding author at: CIFICEN-CONICET,-UNCPBA, Exactas, Pinto 399, Buenos Aires, 7000 Tandil, Argentina. Tel.: +54 249 4439661; fax: +54 249 4439669.
E-mail address: chaparromauro76@gmail.com (M.A.E. Chaparro A.E.).

http://dx.doi.org/10.1016/j.ecolind.2015.02.018
1470-160X/

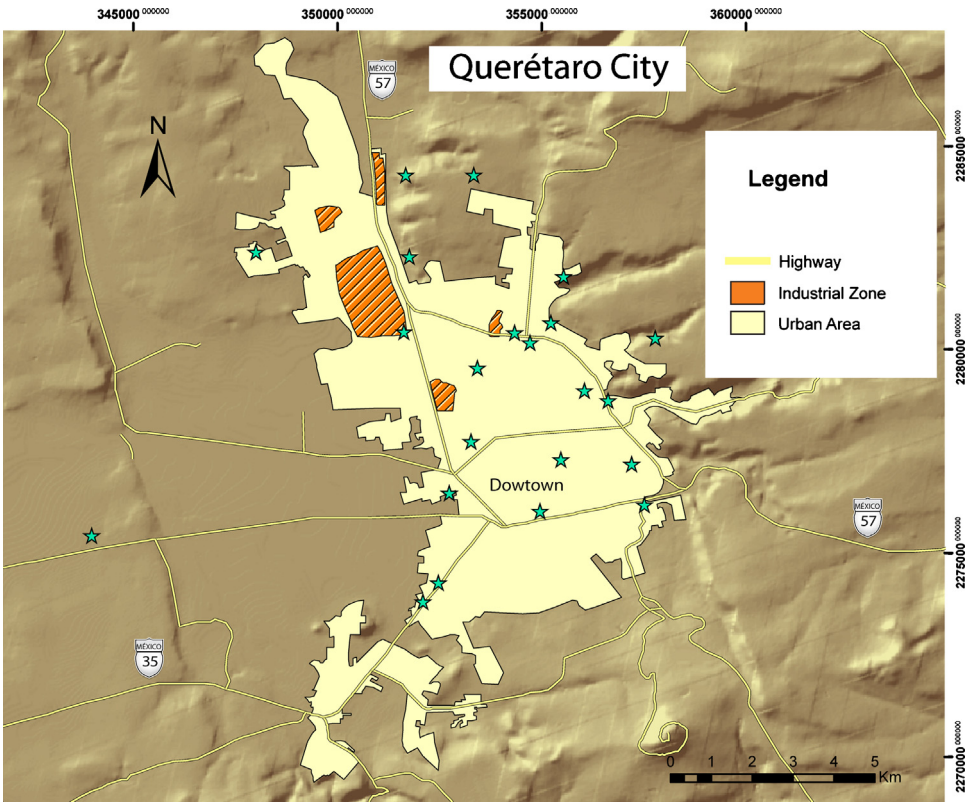

Fig. 1. Study area. Sampling sites in Santiago de Queretaro city (México).

revealing a link between magnetic and chemical variables. There are scarce studies that employed fuzzy tools to analyze such relationships previous to 2010. For example, Hanesch et al. (2001) used fuzzy *c*-means clustering to determine polluted sites in Austria, on the other hand, Kuncheva et al. (2000) proposed a fuzzy model to calculate an index of pollution based on 10 heavy metals loading but they do not used magnetic parameters.

Chaparro et al. (2012) reported a methodology for building an interval fuzzy model for the pollution index PLI (Tomlinson et al., 1980), which was applied to two cases of study, one with soil samples from Antarctica and the other with road-deposited sediments collected in Argentina. The study showed not only satisfactory agreement between the estimation interval and data, but also provided valuable information from the rule analysis, which allows for understanding the magnetic behaviour of the studied variables under different conditions. The work was the first interval model that allows us to calculate the values of index pollution using only magnetic measurements in that sites. Recently, Xia et al. (2014) and Wang et al. (2014) obtained similar results to Chaparro et al. (2011, 2012), but they do not build a mathematical model, they applied fuzzy clustering and principal component analysis to investigate the levels of magnetic and heavy metal contamination of topsoils in China. Their studies reveal a relation between parameters related to magnetic concentration, grain size and mineralogy.

Chaparro et al. (2013) studied lichen species as air pollution biomonitors in urban areas and assessed their potential for magnetic monitoring in cities. They found that samples with industrial influence (heavily polluted sites) showed the highest values in magnetic concentration and coarser magnetic grains. On the contrary, samples from control sites showed the lowest magnetic concentration values, as well as the highest values of grain-size-dependent parameters and hence finer particles.

Mathematical models allow us to derive a more complete and global knowledge from a case study. Fuzzy tools usually are appropriated to combine quantitative (measurements) and qualitative (gained experience) knowledge; this weighted combination enriches the quality of the outcome, giving a better fit between data and modelled results.

Our previous results (Chaparro et al., 2012) encourage us to build a new mathematical model for biomonitors. Thus, in this work, continuing and improving our previous studies, we propose analyzing the relationship between magnetic and chemical variables through the construction of a mathematical model of "fuzzy interval" type or "interval fuzzy model" (IFMo). These types of models are based on fuzzy logic and arithmetic of fuzzy numbers.

2. Materials and methods

2.1. Study area

The Santiago de Querétaro city is the capital of Querétaro de Arteaga state from Mexico. The urban area is about 741 km^2 and has ~800,000 inhabitants (SEDESU, 2006). Based on limited data, there are two hypothesis of the main cause of air pollution in Querétaro, attributed to the vehicles of the city (INEGI, 2003) and to the local industry (Gasca, 2007). The city is located on the intersection of two of the most important routes in Mexico. Highway 57 accommodates most of the north-south traffic between Mexico City and the US border, including also the city of Monterrey. Highway 35D drives traffic in an east-west direction between Mexico City, the Bajío region and the Pacific coast. The city is also host to five large industrial areas which are located in the urban area (Fig. 1). Mean annual precipitation is low, averaging about 570 mm. Vegetation cover is also low; it is composed mostly of steppe shrubs, cacti, and phreatophytes. Wind intensities and directions are also strongly seasonal, with monthly mean velocities of 4 m/s throughout the year. Winds are from the E or NE about 37% of the year, and from

the SW, W or NW about 25% of the time. Winter months may be affected by polar-continental air masses.

2.2. Dataset

The dataset under study was recently submitted for publication to *Ecological Indicators*. Such dataset was obtained by sampling individuals of *T. recurvata* from 26 sites according to their availability in three areas of interest from Querétaro city: industrial, urban and the outskirts. Samples were collected at a height of >1.5 m to avoid the influence of urban soil particles. The material was collected in March 2012, packed in paper bags and stored at room temperature in the laboratory for different magnetic and additional studies. A total of 73 samples of 26 sites were studied.

2.3. Magnetic measurements

The rock-magnetic measurements of biological material were carried out in the laboratory of Paleomagnetism and Rock-magnetism at Centro de Geociencias (UNAM). The material was used for measuring the following parameters:

- The volumetric (κ)and mass-specific (χ) magnetic susceptibility were measured using a KLY-3 Kappabridge meter (AGICO).
- The anhysteretic remanent magnetization (ARM) and the anhysteretic susceptibility (κARM) were determined from the ARM acquired in an alternating field (AF) of 100 mT and a DC bias field of 71.58 A/m (corresponding to an induction of 90 μT). The remanent magnetization was imparted using a laboratory built AF demagnetizer and measured using the magnetometer JR-5.
- The saturation of isothermal remanent magnetization (SIRM = IRM2T) was also produced using a pulse magnetizer, applying a DC field of 2 T, and measured using the above-mentioned magnetometer JR-5.
- The magnetic hysteresis loops and remanent magnetizations were measured in fields between −2 and 2 T at room temperature using a Princeton Measurement Corporation Micromag 2900 AGM system. Among hysteresis parameters and ratios of interest, the saturation magnetization (M_s), saturation remanence (M_{rs}), coercive force (H_c), remanent coercivity (H_{cr}) and the high-field magnetic susceptibility (χhf) were calculated.

In addition, some ratios of interest like as: κ_{ARM}/κ ARM/SIRM SIRM/κ SIRM/χ, H_{cr}/H_c M_{rs}/M_s, the relative contribution of paramagnetic and diamagnetic minerals to the *Ms* (para/diamag. cont.) and S-ratio (=−IRM−300mT/SIRM) were calculated.

On the other hand, the output chemical variable is a composite index of 24 trace and major element concentration.

The Tomlinson pollution load index was calculated with the concentration of 9 heavy metals: Pb, Cr, V, Sn, Sb, Ba, Cu, Zn and Mo, using the following definition:

$$\mathrm{PLI} = \sqrt[n]{\prod_{i=1}^{m}\left(C_{\mathrm{HM},i}/C_{\mathrm{baseline},i}\right)}$$

where $C_{HM,i}$ is the concentration of each heavy metal and $C_{baseline,i}$ is the baseline value for each element (Tomlinson et al., 1980). In this case, the values of baseline were obtained from the minimum values of the dataset for each heavy metal. The values for each chemical element are 41.5 μg/g (Cr), 18.9 μg/g (Ni), 23.4 μg/g (Cu), 144.7 μg/g (Zn), 3.1 μg/g (Mo), 2.9 μg/g (Sn), 1.9 μg/g (Sb), 164.7 μg/g (Ba), 14.0 μg/g (Pb) (Sites A72–73 and A22–24).

2.4. The model, construction and selection methods

2.4.1. Interval fuzzy model, an overview

An interval fuzzy model is a model based on the fuzzy logic and fuzzy set theory. An IFMo consists of two parts basically, "*fuzzy sets*" and "*base of rules*".

This theory was developed by Zadeh (1965); it is particularly useful for the representation of vague expert knowledge and imprecise information about systems.

The fuzzy set theory is based on an extension of the classical meaning of the term "set".

In classical set theory an element "*x*" of an universe *X* either "belongs" or "does not belong" to a set *A*. This concept is represented by the classical "*characteristic function* χ_A":

$$\chi_A(x) = \begin{cases} 1, i\, x \in A \\ 0, \text{ otherwise} \end{cases}$$

The fuzzy set theory rests on the idea that "belongs or does not belong" are particular cases; all elements belong (or do not belong) to a grade of membership. Therefore fuzzy set theory replaces the χ_A with a "*membership function*" $\mu_A(x)$ that represents the degree of membership of *x* to *A*.

$$\mu_A : X \to [01]$$

$$x \underset{\to}{\mu}\, \mu_A(x)$$

The set of pairs $A = \left\{(x, \mu_A(x)), \quad x \in X\right\}$ is called "*fuzzy set*".

The fuzzy sets allow a partition of input and output variables in situations that the expert or modeller has certainty about the problem. The type of membership function represents the uncertainty around these values. Some commonly used membership functions are showed in Fig. 2. For example, in the trapezoidal functions the certainty is along one interval. In case of the triangular or Gaussians function the certainty is on only point but, in the Gaussian function the uncertainty is smoother than the triangular function. The membership functions have two purposes, one is to represent the certainty through the central parameters of functions and the other is to model the uncertainty through of the membership function type.

The other basic part is the base of rules. Each rule is the result of modelling linguistic labels by fuzzy sets. The simplest rules are those

"if *x* is *A* then *y* is *B*"

If the membership functions or rules are not adequate, the assessment of the model will be poor.

2.4.2. The model

The selection of variables was carried out according to the empirical knowledge and relevance of parameters in magnetic monitoring. According to magnetic characteristics, we assumed that three "general" groups of all variables (measured and calculated) are possible to distinguish magnetic group related to: *Concentration* (χ, ARM, M_s, SIRM); *Grain Size* (κ_{ARM}, κ_{arm}/κ, SIRM/χ, ARM/SIRM) and *Mineralogy* (H_{cr}, H_c, χhf). We consider that a model should be built using at least one variable of each magnetic group. Therefore, the parameters selected by the experts were:

Magnetic concentration: mass-specific magnetic susceptibility and the saturation magnetization were selected. The χ is, perhaps, the best and the most used parameter for assessing magnetic concentration in environmental samples, assuming uniform mineralogy and consideration of paramagnetic and diamagnetic components (Peters and Dekkers, 2003). The M_s is considered as

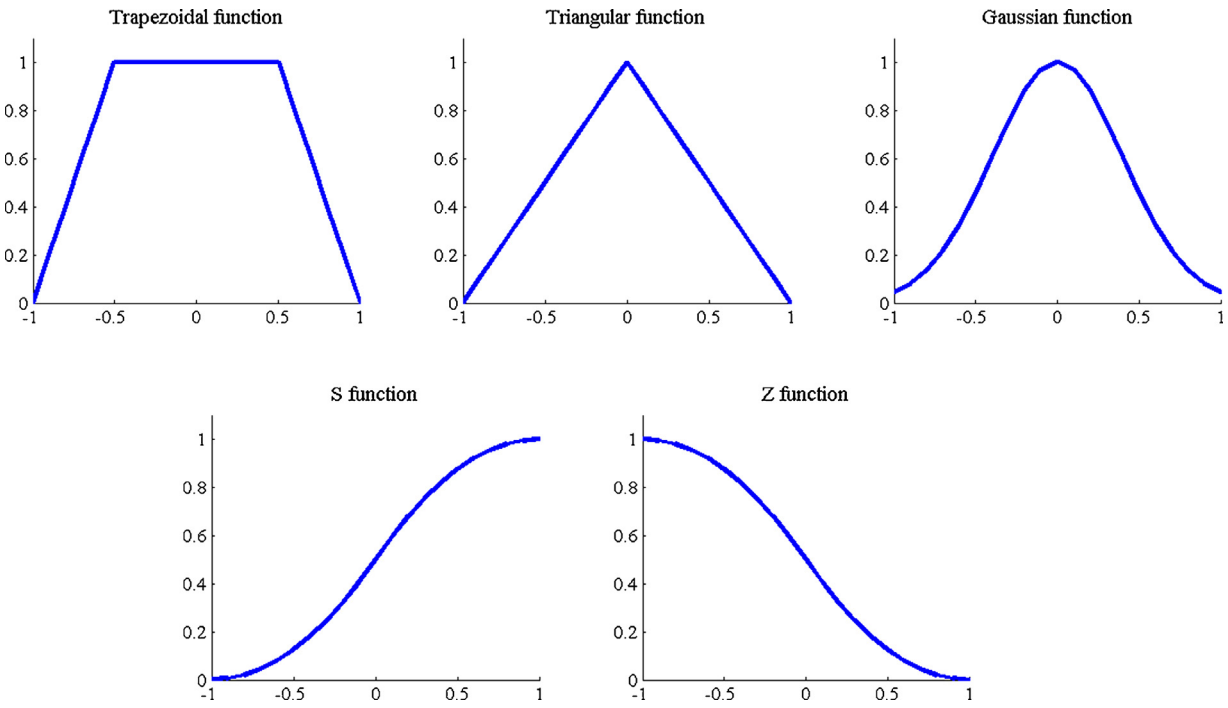

Fig. 2. Membership functions commonly used in fuzzy inference systems.

one of five of the most important hysteresis parameters, which is the magnetization induced in the presence of a large (>1 T) magnetic field.

Magnetic mineralogy: the χhf is the susceptibility in saturating fields (i.e., the high-field slope) and it is frequently used as a proxy for the non-ferrimagnetic contribution to susceptibility, i.e. the combined paramagnetic and diamagnetic contributions.

Magnetic grain size: the κ_{ARM}/κ-ratio is a grain size sensitive parameter (Dunlop and Özdemir, 1997; Peters and Dekkers, 2003), for example, values of κ_{ARM}/κ greater than 5 are indicative of the presence of very small magnetite grains.

The membership functions and rules are built through an unsupervised clustering algorithm that allows finding several partitions ambiguously called fuzzy *c*-means clustering (FCC).

The operations between the fuzzy set are defined by *t-norm* minimum and *t-conorm* maximum for intersection and union respectively. The fuzzy implication or inference is defined by *t-norm* minimum (Mamdani's inference). It is noteworthy that the output of fuzzy inference is a fuzzy set. For practical applications a crisp value is calculated, this process is called *defuzzification.* It is important to quantify the uncertainty of the process that is modelled. Therefore, we think that useful information is lost in classical defuzzification process; for this reason and to achieve better results, a fuzzy interval was calculated instead of a crisp output. The fuzzy arithmetic is used in order to obtain this interval.

A fuzzy interval was defined by a fuzzy set A satisfying the following: (a) A is normal; (b) The support $\{x: A(x) > 0\}$ of A is bounded; (c) The α-cuts of A are closed intervals.

Fuzzy arithmetic is based on two properties of fuzzy numbers: each fuzzy number can fully and uniquely be represented by its α-cuts and the α-cuts of each fuzzy number are closed intervals of real numbers for all $\alpha > (0, 1)$ (Klir and Yuan, 1995). These properties enable us to define arithmetic operations on fuzzy numbers, in terms of operations on closed intervals (Chaparro et al., 2012). The possible results of the model are based on the testing of all rules. These rules must be combined in some manner in order to make a decision. The aggregation method is the process by which the fuzzy sets, which represent the outputs of each rule, are combined into a single fuzzy set. In our model the aggregation method is defined by the average fuzzy interval (or number): $\bar{X}_{fz} = \frac{1}{n}\sum_{i=1}^{n}\alpha_i\tilde{A}_i = \frac{1}{n}\sum_{i=1}^{n}a_i\left(x_i^{Inf}, x_i^{C\ inf}, x_i^{C\ sup}, x_i^{Sup}\right)$ where $\tilde{A}_i$ is a fuzzy set and α_i is the grade of membership of answer i-th fuzzy set.

From this interval fuzzy output, the interval width represents the estimation uncertain. Thus, the model is based on the following hypothesis:

"The response interval width tends to zero when the model is fit".

The inference rules are built using piece of information from the fuzzy partition. From the samples, the maximum membership degree (if above 0.60) of each input and output variables is considered to build a rule. If the membership value is below 0.60, this datum is not used for the rules. It is necessary for all the variables of a sample to have membership grades above 0.60; otherwise the sample will not be used in the model. According to Chaparro et al. (2012), each "useful" sample is identified and labelled using its corresponding fuzzy set with maximum membership. Thus, the rule is established by the label of each set for each variable.

2.4.3. A criterion to select the best model

The all possible models for samples were made up using 23 points of the data pool. For each sample the model architecture was varied from 3 to 5 and 3 to 12 membership functions to input variables and output variables respectively. Therefore the simplest model has 3 input membership functions for the variables χ, M_s, κ_{arm}/κ, and χ_{hf}.

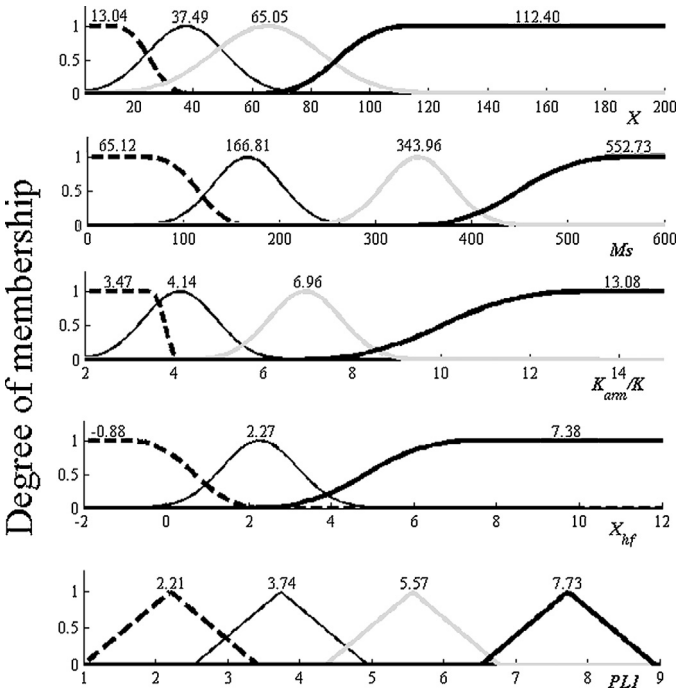

Fig. 3. Membership functions for all variables (input and output). The labels or names for each membership functions are according to the values of the centroid.

Table 1
Statistics resume for the obtained groups by fuzzy *c*-means clustering. The values between brackets are the member number of each fuzzy set.

	Centroid (n)	d.e.	Min	Max
χ				
χ1	13.04 (5)	5.64	1.77	15.32
χ2	37.49 (11)	8.18	19.29	44.12
χ3	65.05 (5)	7.57	46.01	64.54
χ4	112.40 (5)	34.59	81.05	171.54
M_s				
M_s1	65.12 (5)	22.66	25.70	82.60
M_s2	166.81 (14)	42.77	91.90	211.50
M_s3	343.96 (4)	28.10	301.60	367.00
M_s4	552.73 (3)	94.09	498.30	665.90
κ_{ARM}/κ				
κ_{ARM}/κ1	3.47 (3)	0.41	2.89	3.69
κ_{ARM}/κ2	4.14 (14)	0.48	3.17	4.68
κ_{ARM}/κ3	6.96 (7)	1.54	2.50	7.38
κ_{ARM}/κ4	13.08 (2)	3.18	8.73	13.23
χ_{hf}				
χ_{hf}1	−0.88 (11)	1.14	−2.10	1.05
χ_{hf}2	2.27 (8)	0.78	1.52	3.39
χ_{hf}3	7.38 (7)	1.72	5.02	9.00
PLI				
PLI1	2.21 (8)	0.60	1.06	2.94
PLI2	3.74 (12)	0.40	3.18	4.44
PLI3	5.57 (4)	0.49	4.77	5.92
PLI4	7.73 (2)	0.40	7.45	8.02

The fitness measure of the model was defined in order to compare all models. It is defined by the following formula:

$$R_{IF} = \frac{1}{N_i}\sum_{i=1}^{N}\left(2 - \mu_{X_i}(x_i)\right) d\,\mathrm{fuzz}(X_i,\ x_i)$$

where N_i is the number of points that fall into the interval, $d$fuzz(,,) is the distance between to fuzzy numbers (Appendix A), and $\mu_{X_i}(\cdot)$ is the membership function of fuzzy output X_i.

When the fitness is perfect, the value of R_{IF} equals 0. Then, the model is selected from the one that takes the lowest value of R_{IF}.

3. Results

In order to find the best model a total of 460,000 models were built and tested. The lowest value of fitness yielded an $R_{IF} = 0.2064$, corresponding to a model that has 19 rules and 4 membership functions for the input variables χ, M_s, κ_{ARM}/κ, and 3 functions for the input variable χ_{hf}. The output variable PLI has 4 membership functions.

The parameters of the membership function for each variable were determined by a FCC. The group centroids (for each variable) were taken like as the maximum membership value. The membership functions type "*Z*" and "*S*" were used for extreme values of centroids (minimum and maximum) and the Gaussian functions were fitted for middle centroids. This procedure was carried out

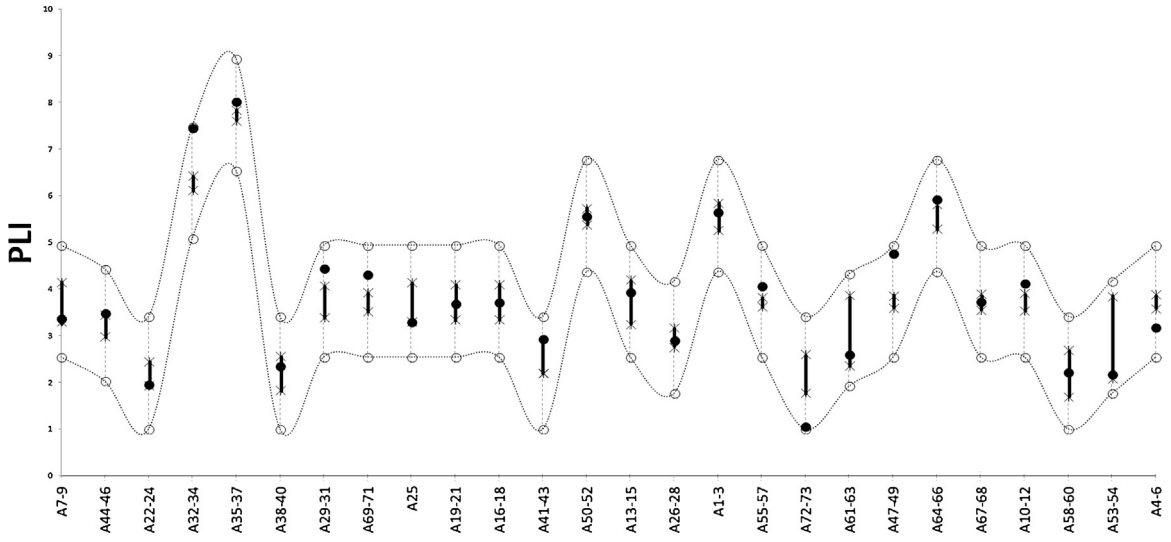

Fig. 4. The outcome of applying the model for the input dataset. The PLI data (•) from the input set. The *center* of the fuzzy interval is denoted with a black line (___) and the *overestimation interval*(◦−*) and *underestimation interval*(*−◦).

Table 2
Type and parameters of the membership functions. The labels or names for each membership functions a roid (*value of maximum membership*) for each partition; e.g. the centroid of PLI1 is lower than PLI2 and so on for all variables.

	Name	Type	Parameters			Name	Type	Parameters		
		INPUT	*A*	*b*			OUTPUT	*a*	*b*	*c*
χ	$\chi 1$	Z(α,β)	13.04	37.49	PLI	PLI1	Tri(a,b,c)	1	2.21	3.41
	$\chi 2$	Gauss(a,b)	13.01	37.49		PLI2	Tri(a,b,c)	2.54	3.74	4.94
	$\chi 3$	Gauss(a,b)	18	65.05		PLI3	Tri(a,b,c)	4.37	5.57	6.77
	$\chi 4$	S(a,b)	65.05	112.4		PLI4	Tri(a,b,c)	6.53	7.73	8.93
M_s	$M_s 1$	Z(a,b)	65.12	166.81						
	$M_s 2$	Gauss(a,b)	18.02	166.81						
	$M_s 3$	Gauss(a,b)	18.05	343.96						
	$M_s 4$	S(a,b)	343.96	552.73						
κ_{ARM}/κ	$\kappa_{ARM}/\kappa 1$	Z(a,b)	3.47	4.14						
	$\kappa_{ARM}/\kappa 2$	Gauss(a,b)	0.8	4.14						
	$\kappa_{ARM}/\kappa 3$	Gauss(a,b)	0.8	6.96						
	$\kappa_{ARM}/\kappa 4$	S(a,b)	6.96	13.08						
χ_{hf}	$\chi_{hf} 1$	Z(a,b)	−0.88	2.27						
	$\chi_{hf} 2$	Gauss(a,b)	0.9	2.27						
	$\chi_{hf} 3$	S(a,b)	2.27	7.38						

only for input variables. The triangular functions were used for output variable. The parameters for these functions were defined by:

$$(\text{centroid} - 2 \times \text{sd},\ \text{centroid}, \text{centroid} + 2 \times \text{sd})$$

where "sd" is the maximum standard deviation of all group belonging to the variable output. All membership functions are shown in Fig. 3 and the centroid, size, standard deviation and minimum–maximum values of each group are summarized in Table 1. All parameters and type of membership functions are detailed in Table 2.

The base for this model is made up of 19 rules; they are showed in Table 3. The set of rules allows us the analysis of, in general terms, the features of samples regarding different levels of pollution, i.e. different values of PLI.

4. Discussion

The outcome of applying the model is shown in Fig. 4. In this figure, the PLI data, modelled values are displayed for comparison purpose. This model has the lowest value of fitness among a total of about half million possible models, which comprised 19 rules and 11 membership functions for the input variables (χ, M_s, κ_{ARM}/κ, χ_{hf}.) and the output variable (PLI).

The interval model contained 96% of PLI values. If we called "overestimation interval" to interval with limit Linf, CenterInf; "underestimation interval": CenterSup, Lsup; and "center": CenterInf, CenterSup (Fig. 4). The values of samples were distributed mostly in the center, that is,

- Overestimation interval: (≈11.5%) A25; A53–54; A72–73.
- Center: (≈53%) A22–24; A53–54; A58–60; A38–40; A61–63; A26–28; A7–9; A19–21; A16–18; A67–68; A13–15; A29–31; A50–52; A1–3.
- Underestimation interval: (≈35.5%) A41–43; A44–46; A55–57; A10–12; A69–71; A47–49; A64–66; A32–34; A35–37.

Besides calculating the value of PLI, the model allows us to do a description and classification of samples in magnetic terms based on the fuzzy rules. As observed in Table 1, the samples with the lowest PLI values (PLI1) (samples A72–73 and A22–24) show low values of magnetic concentration-dependent parameters ($\chi 1$–2 y $M_s 1$), fine magnetic grains ($\kappa_{ARM}/\kappa 3$–4) and low values of high-field magnetic susceptibility ($\chi_{hf} 1$). It is worth mentioning that this χ_{hf} value is related to the concentration of diamagnetic/paramagnetic minerals.

The low-moderate values of magnetic concentration-dependent parameters ($\chi 2$ and $M_s 2$) and slightly coarser (than the previous samples) magnetic grain size ($\kappa_{ARM}/\kappa 2$–3) characterize the samples (A55–57, A47–49, A4–6, A67–68, A10–12, A69–71 and A29–31) with moderate PLI values (PLI2). In this case, the variable χ_{hf} does

Table 3
Base of rules for the interval fuzzy model.

	Input	Output
If	$\chi 1 \wedge M_s 1 \wedge \kappa_{ARM}/\kappa 4 \wedge \chi_{hf} 1$ (1141) $\chi 1 \wedge M_s 2 \wedge \kappa_{ARM}/\kappa 2 \wedge \chi_{hf} 2$ (1222) $\chi 2 \wedge M_s 1 \wedge \kappa_{ARM}/\kappa 3 \wedge \chi_{hf} 1$ (2131) $\chi 2 \wedge M_s 2 \wedge \kappa_{ARM}/\kappa 3 \wedge \chi_{hf} 1$ (2231) $\chi 2 \wedge M_s 2 \wedge \kappa_{ARM}/\kappa 3 \wedge \chi_{hf} 2$ (2232) $\chi 4 \wedge M_s 2 \wedge \kappa_{ARM}/\kappa 3 \wedge \chi_{hf} 1$ (4231)	Then PLI1 (lowest values)
If	$\chi 1 \wedge M_s 2 \wedge \kappa_{ARM}/\kappa 2 \wedge \chi_{hf} 1$ (1221) $\chi 2 \wedge M_s 1 \wedge \kappa_{ARM}/2 \wedge \chi_{hf} 1$ (2121) $\chi 2 \wedge M_s 2 \wedge \kappa_{ARM}/\kappa 2 \wedge \chi_{hf} 1$ (2221) $\chi 2 \wedge M_s 2 \wedge \kappa_{ARM}/\kappa 2 \wedge \chi_{hf} 2$ (2222) $\chi 2 \wedge M_s 3 \wedge \kappa_{ARM}/\kappa 2 \wedge \chi_{hf} 3$ (2323) $\chi 3 \wedge M_s 2 \wedge \kappa_{ARM}/\kappa 2 \wedge \chi_{hf} 2$ (3222) $\chi 3 \wedge M_s 4 \wedge \kappa_{ARM}/\kappa 2 \wedge \chi_{hf} 3$ (3423) $\chi 4 \wedge M_s 2 \wedge \kappa_{ARM}/\kappa 2 \wedge \chi_{hf} 2$ (4222)	Then PLI2
If	$\chi 1 \wedge M_s 2 \wedge \kappa_{ARM}/\kappa 2 \wedge \chi_{hf} 1$ (1221) $\chi 2 \wedge M_s 1 \wedge \kappa_{ARM}/2 \wedge \chi_{hf} 1$ (2121) $\chi 2 \wedge M_s 2 \wedge \kappa_{ARM}/\kappa 2 \wedge \chi_{hf} 1$ (2221)	Then PLI3
If	$\chi 1 \wedge M_s 2 \wedge \kappa_{ARM}/\kappa 3 \wedge \chi_{hf} 2$ (1232) $\chi 4 \wedge M_s 3 \wedge \kappa_{ARM}/\kappa 2 \wedge \chi_{hf} 3$ (4323)	Then PLI4 (highest values)

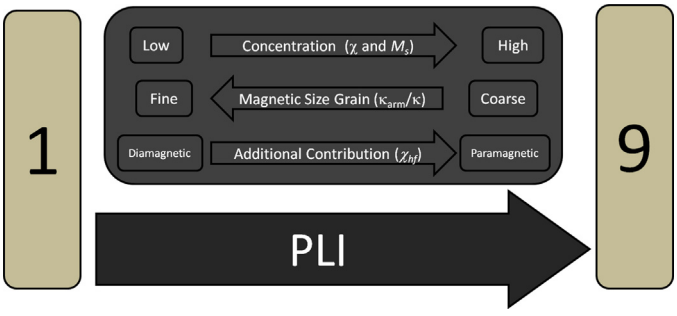

Fig. 5. A conclusion about the PLI increasing. An analysis using the base of rules for the interval fuzzy model.

not show a particular feature, all fuzzy sets were observed for this PLI value, i.e. $\chi_{hf}1$–2–3.

All samples with higher PLI values (PLI3 and PLI4) showed higher values of high-field magnetic susceptibility ($\chi_{hf}3$) and high values of magnetic concentration-dependent parameters ($\chi 3$–4 and $M_s 3$). In addition, most of the samples have coarser magnetic grain sizes ($\kappa_{ARM}/\kappa 1$–2).

5. Conclusions

The model is a very good approximation of the case of study that allows the use of magnetic parameters for future biomonitoring studies at low cost.

The model yields a satisfactory approximation of (measured) data for PLI. This fact is reflected in results of R_{IF} indicator (0.2064) used.

The interval model contained 96% of PLI values. These values were distributed in the overestimation interval (≈11.5%), center: (≈53%) and underestimation interval: (≈35.5%).

After analyzing the rules, it was concluded that the PLI increases with relation to:

- an increase in concentration of magnetic materials and
- an additional contribution to the magnetic signal of paramagnetic materials and
- an increase in size of the magnetic grains (Fig. 5).

Thus the model allows us to identify how the magnetic variables were affected, in the transition, from unpolluted to more polluted sites.

It is expected that the accuracy of the model (interval width) will be improved adding new samples to the dataset. In particular, it is very important to include "extreme" samples (i.e.: samples belonging to pristine zones and with high pollution loading) in order to reinforce the base and strengthen the features of these samples. It is worth notice that in this dataset only two samples take a PLI < 2 (A22–24 and A72–73). Despite this fact, the obtained rules for these PLI values are according to previous studies (Chaparro et al., 2011, 2012).

A final observation about the position of the samples: it is observed that the samples with low PLI values correspond to zones with fluid vehicular traffic (high speed highways). The samples corresponding to the highest PLI values are located in industrials zones or zones with high vehicular traffic at low speed (e.g. city center or school zones).

Acknowledgements

This research was partly supported by Posgrado en Ciencias de la Tierra (UNAM). The authors wish to thank the UNAM, UNCPBA and CONICET for their financial support. This manuscript was improved by useful suggestions by two anonymous reviewers.

Appendix A. Distance between two trapezoidal fuzzy numbers

Definition 1: Let A a fuzzy set is called "trapezoidal fuzzy number" if:

(1) $\forall\alpha \in [01]$, A_α is a convex set on R.

(2) The membership function of A is:

$$\mu_A(x) = \begin{cases} \dfrac{x - L_A}{-C_{LA} - L_A} & \text{when } L_A \le x \le C_{LA} \\ 1 & \text{when } C_{LA} \le x \le C_{SA} \\ \dfrac{S_A - x}{S_A - C_{SA}} & \text{when } C_{SA} \le x \le S_A \\ 0 & \text{otherwise} \end{cases}$$

where A^L, A^{C1}, A^{C2}, A^R are the parameters of A.

Definition 2: Let A and B two flat fuzzy numbers. The distance between two fuzzy numbers is defined by:

$$d(A,B) = \int_0^1 f(\alpha)\, d^2(A_\alpha, B_\alpha)\, d\alpha$$

where $d^2(A_\alpha, B_\alpha) = \left(\underline{A_\alpha} - \underline{B_\alpha}\right)^2 + \left(\bar{A_\alpha} - \bar{B_\alpha}\right)^2$ and $\underline{A_\alpha} = a\left(A^{c1} - A^L\right) + A^L$; $\bar{A}_\alpha = A^s - \alpha\left(A^s - A^{C2}\right)$.

The $f(\alpha)$ is a monotonously increasing function at [0,1], and $f(0) = 0$; $\int_0^1 (\alpha)\, d\alpha = \frac{1}{2}$ (Bing-Yuan Co, 2006).

Proposition: Let A and B two trapezoidal fuzzy numbers with membership functions according to *Definition 1*. Then according to *Definition 3*, if $f(\alpha) = \alpha$. The distance between trapezoidal fuzzy numbers is defined by:

$$\begin{aligned} d(A,B) = {} & \frac{2(S_A - S_B)((C_{SB} - C_{SB}) - (S_A - S_B))}{3} \\ & + \frac{((C_{LA} - C_{LB}) - (L_A - L_B))^2}{4} + \frac{((C_{SA} - C_{SB}) - (S_A - S_B))^2}{4} \\ & + \frac{(S_A - S_B)^2 + (L_A - L_B)^2}{2} \\ & + \frac{2(L_A - L_B)((C_{LB} - C_{LB}) - (L_A - L_B))}{3} \end{aligned}$$

Proof:

The α-cut to trapezoidal fuzzy number is define by $A_\alpha = \left[\underline{A_\alpha}, \bar{A_\alpha}\right]$ where

$$\underline{A_\alpha} = L + \alpha(C_{LA} - L_A) \text{ and } \bar{A_\alpha} = S_A + \alpha(C_{SA} - S_A)$$

Applied the *definition 2* the expression of the distance is:

$$d(A,B) = \int_0^1 f(\alpha)\, d^2(A_\alpha, B_\alpha)\, d\alpha = \int_0^1 \alpha\left(\left(\underline{A_\alpha} - \underline{B_\alpha}\right)^2 + \left(\bar{A_\alpha} - \bar{B_\alpha}\right)^2\right) d\alpha =$$

$$\int_0^1 \alpha\left(((L_A + \alpha(C_{LA} - L_A)) - (L_B + \alpha(C_{LB} - L_B)))^2 + ((S_A + \alpha(C_{SA} - S_A)) - (S_B + \alpha(C_{SB} - S_B)))^2\right) d\alpha$$

$$= \frac{((A_C - A_L) - (B_C - B_L))^2}{4} + \frac{((A_C - A_S) - (B_C - B_S))^2}{3} + \frac{(A_L - B_L)^2}{2} + (A_S - B_S)^2 + \frac{2(A_L - B_L)((A_C - A_L) - (B_C - B_L))}{3} + (A_S - B_S)((A_C - A_S) - (B_C - B_S))$$

Appendix B. Supplementary data

Supplementary data associated with this article can be found, in the online version, at http://dx.doi.org/10.1016/j.ecolind.2015.02.018.

References

Aguilar-Reyes, B., Cejudo Ruiz, R., Martínez-Cruz, J., Bautista, F., Goguitchaichvili, A., Carvallo, C., Morale, J., 2012. *Ficus benjamina* leaves as indicator of atmospheric pollution: a reconnaissance study. Stud. Geophys. Geod. 56, 879–887.

Bing-Yuan Cao., 2006. Studies in Fuzziness and Soft Computing, Springer-Verlag, Berlin Heidelberg.

Castañeda-Miranda, A.G., Bhônel, H., Molina-Garza R.S., Chaparro, M.A.E., 2014. Magnetic evaluation of TSP-filters for air quality monitoring. Atmos. Environ. 96, 163–174.
Castañeda-Miranda, A.G., 2014. Caracterización y monitoreo Magnético ambiental de Partículas suspendidas en el aire Urbano. Universidad nacional Autónoma de México, México (Tesis Doctorado).
Chaparro, M.A.E., Gogorza, C.S.G., Chaparro, M.A.E., Irurzun, M.A., Sinito, A.M., 2006. Review of magnetism and pollution studies of various environments in Argentina. Earth Planets Space 58 (10), 1411–1422.
Chaparro, M.A.E., Nuñez, H., Lirio, J.M., Gogorza, C.G.S., Sinito, A.M., 2007. Magnetic screening and heavy metal pollution studies in soils from Marambio station, Antarctica. Antarct. Sci. 19 (3), 379–393.
Chaparro, M.A.E., Chaparro, M.A.E., Marinelli, C., Sinito, A.M., 2008. Multivariate techniques as alternative statistical tools applied to magnetic proxies for pollution: cases of study from Argentina and Antarctica. Environ. Geol. 54, 365–371.
Chaparro, Mauro, Chaparro, Marcos, Sinito, Ana, 2011. A fuzzy model for estimating heavy metals in an antartic soil. Latinmag Lett. 1 (2), 1–6 (D34, Proceedings Tandil, Argentina).
Chaparro, M.A.E., Chaparro, M.A.E., Sinito, A.M., 2012. An interval fuzzy model for magnetic monitoring: estimation of a pollution index. Environ. Earth Sci. 66 (5), 1477–1485.
Chaparro, M.A.E., Lavornia, J., Chaparro, M.A.E., Sinito Ana, M., 2013. Biomonitors of urban air pollution: magnetic studies and SEM observations of corticolous foliose and microfoliose lichens and their suitability for magnetic monitoring. Environ. Pollut. 172, 61–69.
Desenfant, F., Petrovský, E., Rochette, P., 2004. Magnetic signature of industrial pollution of stream sediments and correlation with heavy metals: case study from South France. Water Air Soil Pollut. 152 (1), 297–312.
Dunlop, D.J., Özdemir, Ö., 1997. Rock Magnetism. Fundamentals and Frontiers. Cambridge University Press, Cambridge, pp. 573.
Evans, M.E., Heller, F., 2003. Environmental Magnetism. Principles and Applications of Enviromagnetics. Academic Press. An Imprint of Elsevier Science, USA, pp. 299.
Fabian, K., Reimann, C., McEnroe, S.A., Willemoes-Wissing, B., 2011. Magnetic properties of terrestrial moss (*Hylocomium splendens*) along a north–south profile crossing the city of Oslo, Norway. Sci. Total Environ. 409, 2252–2260.
Flanders, P.J., 1994. Collection, measurement, and analysis of airborne magnetic particulates from pollution in the environment. J. Appl. Phys. 75 (10), 5931–5936.
Gasca, M., 2007. Caracterización por SEMEDS de aeropartículas antrópicas de la fracción respirable en la Ciudad de Querétaro y su relación con fuentes contaminantes. Universidad Autónoma de Qurétatro, Universidad Autónoma de Qurétatro (Tesis).
Gautam, P., Blahab, U., Appel, E., 2005. Magnetic susceptibility of dust-loaded leaves as a proxy of traffic-related heavy metal pollution in Kathmandu city, Nepal. Atmos. Environ. 39, 2201–2211.
Georgeaud, V.M., Rochette, P., Ambrosi, J.P., Vandamme, D., Williamson, D., 1997. Relationship between heavy metals and magnetic properties in a large polluted catchment: the Etang de Berre (South of France). Phys. Chem. Earth 22 (1–2), 211–214.
Hanesch, M., Scholger, R., Dekkers, M.J., 2001. The application of fuzzy *c*-means cluster analysis and non-linear mapping to a soil data set for the detection of polluted sites. Phys. Chem. Earth, A 26 (11–12), 885–891.
Hanesch, M., Scholger, R., Rey, D., 2003. Mapping dust distribution around an industrial site by measuring magnetic parameters of tree leaves. Atmos. Environ. 37, 5125–5133.
Instituto Nacional de Estadística Geográfica e informática INEGI, 2003. Anuario Estadístico Querétaro de Arteaga. Instituto Nacional de Estadística Geográfica e informática INEGI, México.
Jordanova, N.V., Jordanova, D.V., Veneva, L., Andorova, K., Petrovský, E., 2003. Magnetic response of soils and vegetation to heavy metal pollution—a case of study. Environ. Sci. Technol. 37, 4417–4424.
Jordanova, D., Petrov, P., Hoffmann, V., Gocht, T., Panaiotu, C., Tsacheva, T., Jordanova, N., 2010. Magnetic signature of different vegetation species in polluted environment. Stud. Geophys. Geod. 54, 417–442.
Kapicka, A., Petrovský, E., Ustjak, S., Macháčková, K., 1999. Proxy mapping of fly-ash pollution of soils around a coal-burning power plant: a case study in Czech Republic. J. Geochem. Explor. 66, 291–297.
Klir, G.J., Yuan, B., 1995. Fuzzy Sets and Fuzzy Logic: Theory and Applications. Prentice Hall, Upper Saddle River, NJ.
Kukier, U., Fauziah Ishak, C., Summer, M.E., Miller, W.P., 2003. Composition and element solubility of magnetic and non-magnetic fly ash fractions. Environ. Pollut. 123, 255–266.
Kuncheva, L.I., Wrench, J., Jain, L.C., Al-Zaidan, A.S., 2000. A fuzzy model of heavy metal loadings in Liverpool bay. Environ. Modell. Softw. 15 (2), 161–167.
Lehndorff, E., Urbat, M., Schwark, L., 2006. Accumulation histories of magnetic particles on pine needles as function of air quality. Atmos. Environ. 40, 7082–7096.
Lu, S.-G., Bai, S.-Q., Cai, J.-B., Xu, C., 2005. Magnetic properties and heavy metal contents of automobile emission particulates. J. Zhejiang Univ. Sci. 6B (8), 731–735.
Maher, B.A., Moore, C., Matzka, J., 2008. Spatial variation in vehicle-derived metal pollution identified by magnetic and elemental analysis of roadside tree leaves. Atmos. Environ. 42, 364–373.
Marié, D.C., Chaparro, M.A.E., Gogorza, C.S.G., Navas, A., Sinito, A.M., 2010. Vehicle-derived emissions and pollution on the road Autovia 2 investigated by rock-magnetic parameters: a case of study from Argentina. Stud. Geophys. Geod. 54, 135–152.
Matzka, J., Maher, B.A., 1999. Magnetic biomonitoring of roadside tree leaves: identification of spatial and temporal variations in vehicle-derived particulates. Atmos. Environ. 33, 4565–4569.
Moreno, E., Sagnotti, L., Dinares-Turell, J., Winkler, A., Cascella, A., 2003. Biomonitoring of traffic air pollution in Rome using magnetic properties of tree leaves. Atmos. Environ. 37, 2967–2977.
Morton-Bermea, O., Hernandez, E., Martinez-Pichardo, E., Soler-Arechalde, A.M., Lozano Santa-Cruz, R., Gonzalez-Hernandez, G., Beramendi-Orosco, L., Urrutia-Fucugauchi, J., 2009. Mexico City topsoils: heavy metals vs. magnetic susceptibility. Geoderma 151, 121–125.
Ng, S.L., Chan, L.S., Lam, K.C., Chan, W.K., 2003. Heavy metal contents and magnetic properties of playground dust in Hong Kong. Environ. Monit. Assess. 89, 221–232.
Peters, C., Dekkers, M., 2003. Selected room temperature magnetic parameters as a function of mineralogy, concentration and grain size. Phys. Chem. Earth 28, 659–667.
Petrovský, E., Kapicka, A., Zapletal, K., Sebestová, E., Spanilá, T., Dekkers, M.J., Rochette, P., 1998. Correlation between magnetic properties and chemical composition of lake sediments from northern Bohemia. Preliminary study. Phys. Chem. Earth, A 23 (9–10), 1123–1126.
Petrovský, E., Kapicka, A., Jordanoa, N., Knob, M., Hoffmann, V., 2000. Low field susceptibility: a proxy method of estimating increased pollution of different environmental systems. Environ. Geol. 39 (3–4), 312–318.
Salo, H., Bucko, M.S., Vaahtovuo, E., Limo, J., Mäkinen, J., Pesonen, L.J., 2012. Biomonitoring of air pollution in SW Finland by magnetic and chemical measurements of moss bags and lichens. J. Geochem. Explor. 115, 69–81.
SEDESU (Secretaría de Desarrollo Sustentable), 2006. Anuario Económicode Querétaro. SEDESU (Secretaría de Desarrollo Sustentable), Disponible en: ⟨http://www.queretaro.gob.mx/sedesu/deseco/esteco/perfeco/anuario/2006/index.htm⟩.
Spiteri, C., Kalinski, V., Rösler, W., Hoffmann, V., Appel, E., MAGPROX Team, 2005. Magnetic screening of a pollution hotspot in the Lausitz area, Eastern Germany: correlation analysis between magnetic proxies and heavy metal contamination in soils. Environ. Geol. 49, 1–9.
Tomlinson, D.L., Wilson, J.G., Harris, C.R., Jeffrey, D.W., 1980. Problems in the assessment of heavy metals levels in estuaries and the formation of a pollution index. Helgol. Meeresunters. 33, 566–575.
Wang, B., Xia, D.S., Yu, Y., Jia, J., Xu, S.J., 2014. Detection and differentiation of pollution in urban surface soils using magnetic properties in arid and semi-arid regions of northwestern China. Environ. Pollut. 184, 335–346.
Wannaz, E.D., Carreras, H.A., Pérez, C.A., Pignata, M.L., 2006. Assessment of heavy metal accumulation in two species of *Tillandsia* in relation to atmospheric emission sources in Argentina. Sci. Total Environ. 361, 267–278.
Xia, D., Wang, B., Yu, Y., Jia, J., Nie, Y., Wang, X., Xu, S., 2014. Combination of magnetic parameters and heavy metals to discriminate soil-contamination sources in Yinchuan—a typical oasis city of Northwestern China. Sci. Total Environ. 485–486, 83–92.
Zadeh, L.A., 1965. Fuzzy Sets. Inf. Control 8, 338–353.
Zhang, C.X., Huang, B.C., Piper, J.D.A., Luo, R.S., 2008. Biomonitoring of atmospheric particulate matter using magnetic properties of *Salix matsudana* tree ring cores. Sci. Total Environ. 393, 177–190.
Zhang, C.X., Quiao, Q., Appel, E., Huang, B.C., 2012. Discriminating sources of anthropogenic heavy metals in urban street dusts using magnetic and chemical methods. J. Geochem. Explor. 119–120, 60–75.